

CALCULATIONS ON A TURBULENT HETEROGENEOUS JET ENTERING  
A HALF SPACE

G. F. Gorshkov and V. S. Terpigor'ev

UDC 532.517.4:533.951.7

Integral equations have been used in calculations on turbulent nonisothermal jets of variable composition escaping into a space filled with air. The calculations are in satisfactory agreement with experiment.

1. Consider an isobaric turbulent jet of viscous compressible gas whose equivalent shock-wave temperature at the end of the nozzle is about  $10^4$ °K and which enters a space filled with different gas. This is a highly nonisothermal jet of variable composition. An example is provided by a low-temperature plasma jet.

The effective boundary-layer thicknesses are the following: dynamic,  $\delta$ ; thermal,  $\delta_T$ ; and diffusion,  $\delta_D$ . Then we can use the conditions for the following fluxes to be zero at the boundary: the momentum  $\rho u^2$ , the excess heat content  $\rho u \Delta h$ , and the excess matter  $\rho u \Delta \xi$ .

Then the differential equations for continuity, momentum, energy, and matter give us that the following integral equations apply:

$$2\pi \int_0^{\delta} \rho u^2 r dr = \pi r_a^2 (\rho u^2)_a, \quad (1)$$

$$2\pi \int_0^{\delta_T} \rho u \Delta H r dr = \pi r_a^2 (\rho u \Delta H)_a, \quad (2)$$

$$2\pi \int_0^{\delta_D} \rho u \Delta \xi r dr = \pi r_a^2 (\rho u \Delta \xi)_a, \quad (3)$$

$$\frac{d}{dx} \int_0^{\delta} \rho u^2 r dr = -2 \int_0^{\delta} \tau_r \frac{\partial u}{\partial r} r dr. \quad (4)$$

Equations (1)-(4) are as follows: (1)-(3) apply for the origin moments and for the first moment, derived from generalized integral equations [1] analogous to Golubev's relations for an incompressible fluid.

For a subsonic jet of moderate speed ( $M_a < 0.5$ )  $h \gg u^2/2$ ; we can therefore assume that  $H \approx h$ .

To (1)-(4) we must add expressions for the dimensionless distributions of  $\rho u^2$ ,  $\rho u \Delta h$ ,  $\rho u \Delta \xi$  together with the equation of state for the mixture of gases and the relationship between the effective thicknesses of the boundary layers.

The following functional relations have been derived [2] for the fluxes of momentum and excess heat content in cross sections of a jet of low-temperature plasma:

$$\frac{\rho u^2}{(\rho u^2)_m} = (1 - \eta^{1.5})^4, \quad (5)$$

$$\frac{\rho u \Delta h}{(\rho u \Delta h)_m} = (1 - \eta_r^{1.5})^4. \quad (6)$$

TABLE 1. Numerical Values of  $A_i$  and  $n_i$  Appearing in the Equation of State

Gas	Air	N <sub>2</sub>	Ar	He	H <sub>2</sub>
$n$	0,8230	0,8345	1	1	0,7851
$A, \text{J/m}^3$	36300	37168	253000	245000	11075
$T \cdot 10^{-3}$	0,29-7,0	0,29-7,0	0,29-9,5	0,29-9,5	0,29-6,0
$\sigma$	0,03	0,07	0,011	0,003	0,004

By analogy with (5) and (6), we have the following for the dimensionless distribution of the excess-matter flux:

$$\frac{\rho u \Delta \xi}{(\rho u \Delta \xi)_m} = (1 - \eta_D^{1,5})^4. \quad (7)$$

We envisage a binary mixture of chemically unreactive gases to which the following equation of state applies:

$$\rho_i = A_i / h_i^{n_i}, \quad (8)$$

The  $A_i$  and  $n_i$  are constants dependent on the nature of component  $i$ . The available data [3] provide these constants. Table 1 gives the numerical values;  $T \cdot 10^{-3}$  is the temperature range for which (8) applies, while  $\sigma$  is the standard deviation of the data of [3] from (8).

We now introduce the relative mass concentration and relative volume of component  $i$ ; then published equations [4] provide the basis for calculations on a binary mixture whose density obeys (8), i.e., we can find the density as a function of the enthalpy and concentration.

Calculations have been performed in this way for a mixture of Ar, He, or N<sub>2</sub> with air, in each case for various concentrations.

The results indicate the following equation of state for the mixture:

$$\rho_m = \frac{A_1}{h_m^{n_1}} \frac{1}{\xi_1 + B h_m^{(n_2 - n_1)} (1 - \xi_1)}, \quad (9)$$

where  $B = A_1/A_2$  and the subscripts 1 correspond to the gas from the nozzle and 2 to the gas in the space. In what follows the subscripts to  $\rho$ ,  $h$ , and  $\xi$  are omitted.

Equation (9) allows one to assume any gas as the filling for the external space.

The differences in the effective thicknesses of the boundary layers are such [2, 5, 6] that we may assume that the thermal and diffusion boundaries coincide, while the relation between  $\delta$ ,  $\delta_T$ , and  $\delta_D$  is [2]

$$\delta_D \simeq \delta_T \simeq \delta / 0.87. \quad (10)$$

In addition, we need an expression for the turbulent friction that appears in (4).

We assume that

$$\tau_r = \rho \nu_r \frac{\partial u}{\partial r} = \rho \kappa \delta u_m \frac{\partial u}{\partial r}. \quad (11)$$

The universal constant  $\kappa$  is taken as 0.0095 for an incompressible fluid [1].

Therefore, the parameters of this jet may be found by solving (1)-(4) with (9) and (10) in conjunction with (5)-(7) and (11) subject to the initial conditions

$$\bar{x} = \bar{x}_0 = x_0/r_0 = 0, \quad \bar{\delta} = \bar{\delta}_0 = \delta_0/r_0.$$

As for  $\bar{x} = \bar{x}_0$  we have  $\overline{(\rho u^2)}_m = (\rho u^2)_m / (\rho u^2)_0 = 1$ ; we get the result for  $\bar{\delta}_0$  from (1) and (5) as

$$\bar{\delta}_0 = 1/(2D)^{0.5} \simeq 2.7367,$$

$$D = \int_0^1 (1 - \eta^{1.5})^4 \eta d\eta = \frac{243}{3640}.$$

This system of equations gives us  $\delta$ ,  $\delta_T$ ,  $\delta_D$ ,  $\rho$ ,  $u$ ,  $h$ ,  $\xi$ .

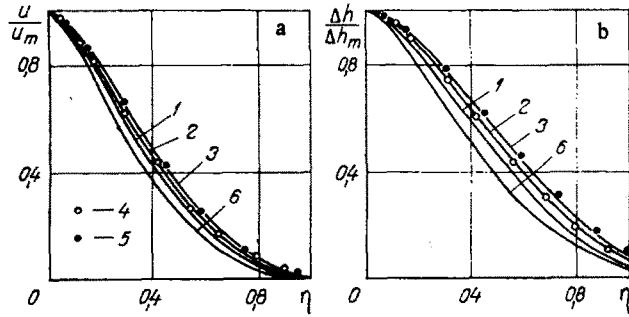


Fig. 1

Fig. 1. Distributions of: a) velocity; b) excess enthalpy in  $N_2$  jets with  $\theta_\alpha = 83.8$ , calculation: 1)  $\bar{x} = 4$ ; 2) 45; 3) 64; experiment: 4)  $\bar{x} = 45$ ; 5) 64;  $\theta_\alpha = 138$ , He, calculation: 6)  $\bar{x} = 4$ .

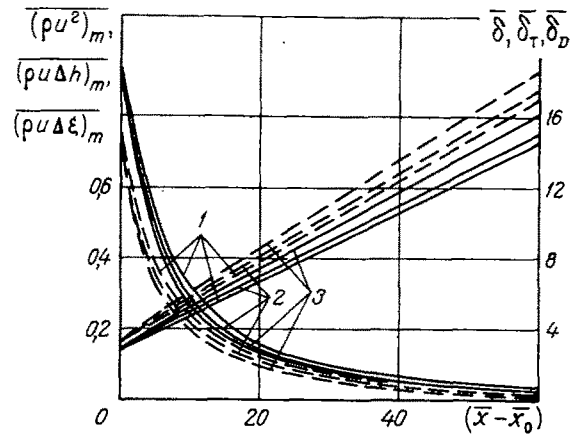


Fig. 2

Fig. 2. Distribution of the fluxes of momentum, excess enthalpy, and matter along the jet axis and the corresponding effective thicknesses in relation to superheating for He and  $\kappa = 0.0095$ ; solid lines from calculation for  $(\rho u^2)_m$  and  $\bar{\delta}$ ; broken lines for  $(\rho u \Delta h)_m$ ,  $(\rho u \Delta \xi)_m$  and  $\bar{\delta}_T$ ,  $\bar{\delta}_D$ : 1)  $\theta_\alpha = 5.3$ ; 2) 16; 3) 138.

2. System (1)-(4) with (9) and (10) was solved with a BESM-4 computer (TA-1M compiler) with an Algol-60 program. The run time for a single case covering the range in  $\bar{x}$  from 0 to 70 was 1 h (including compilation).

Figures 1-3 show some results for jets of argon, helium, and nitrogen entering air with  $\kappa = 0.0095$  for a wide range of excess temperatures  $\theta_\alpha = h_\alpha/h_H$  in the jet.

Qualitatively speaking, the calculations give a physically correct picture for the jet propagation.

For example, the velocity distribution (Fig. 1a) or the excess-enthalpy distribution (Fig. 1b) is not self-modeling and becomes flatter as  $\bar{x}$  increases. This is due to the reduction in the local superheating of the jet.

Under otherwise equal conditions, a jet having a large  $\theta_\alpha$  cools much more rapidly (curves 1 and 6 for  $\bar{x} = 4$  in Fig. 1a and b), i.e., the distributions for  $u$  and  $\Delta h$  become steeper.

The same applies to the axial parameters of the jet, i.e., the falls in  $(\rho u^2)_m$ ,  $(\rho u \Delta h)_m = (\rho u \Delta h)_m / (\rho u \Delta h)_\alpha$ ,  $(\rho u \Delta \xi)_m = (\rho u \Delta \xi)_m / (\rho u \Delta \xi)_\alpha$  for the hotter jets are more rapid, while the effective boundary-layer thicknesses increase, as Fig. 2 shows. The falls in  $(\rho u \Delta h)_m$  and  $(\rho u \Delta \xi)_m$  are steeper than the fall in  $(\rho u^2)_m$  by 0.75.

Figure 3a shows numerical results for the compressibility parameter  $\omega = \rho_H / \rho_\alpha$ , while Fig. 3b shows the results for  $\theta_\alpha$  as regards the expansion of the main part of the jet, that is,  $C = \bar{d}\delta_0 / d\bar{x}$ .

Figure 3a has line 1 as the numerical result for the effect of  $\omega$  on  $C/C_{\omega=1}$  for helium and argon jets, while line 2 represents jets of nitrogen, air, or hydrogen, where the symbols show the experimental results of [2, 5-8].

Clearly, the expansion of the main part of the jet is influenced not only by the compressibility but also by the nature of the gas, and therefore some generalizations in terms of  $\omega$  or  $C$  are not universal.

On the other hand, the superheating parameter  $\theta_\alpha$  (Fig. 3b) provides a close fit to the measurements as a single relationship of the form

$$C/C_{\theta_\alpha=1} = 1 + 0.156 \lg \theta_\alpha. \quad (12)$$

The line calculated from (12) in Fig. 3b fits the numerical results to  $\sigma = 0.02$  for jets of helium, argon, nitrogen, and air escaping into air, while the symbols show measured data from the same sources (symbols as in Fig. 3a). It is clear that the measurements fit the calculations from (12) to  $\sigma = 0.022$ .

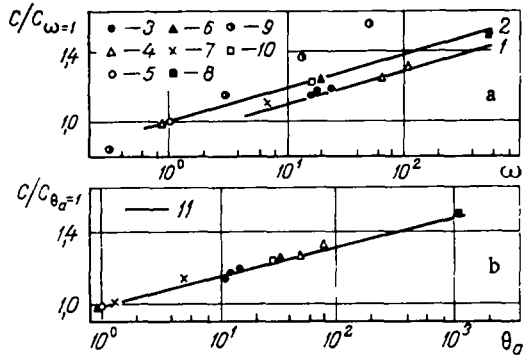


Fig. 3

Fig. 3. Effects of: a) compressibility; b) superheating on the expansion of the main part of the jet: a) calculation: 1) He, Ar; 2) air, N<sub>2</sub>, H<sub>2</sub>; experiment: 3, 4, 5, 6) Ar, He, air, N<sub>2</sub> [2]; 7) [5]; 8) [6]; 9) [7]; 10) [8]; b) calculation: 11) from (12); experiment: 3, 4, 5, 6, 7, 8, 9, 10.

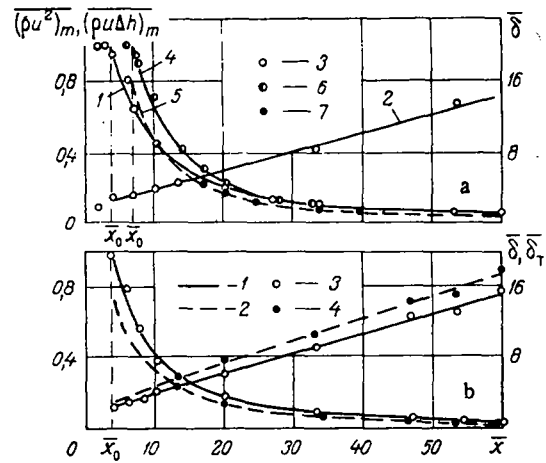


Fig. 4

Fig. 4. Comparison of theory and experiment for the distribution of the axial parameters and the corresponding effective thicknesses; a) Ar,  $\theta_a = 11$ , calc.: 1)  $(\rho u^2)_m$ ; 2)  $\bar{\delta}$ ; experiment: 3)  $(\rho u^2)_m$ ,  $\bar{\delta}$ ; air,  $\theta_a = 26.3$ , calc.: 4)  $(\rho u^2)_m$ ; 5)  $(\rho u \Delta h)_m$ ; experiment: 6)  $(\rho u^2)_m$ ; 7)  $(\rho u \Delta h)_m$  [8]; b) N<sub>2</sub>,  $\theta_a = 29.5$ , calc.: 1)  $(\rho u^2)_m$  and  $\bar{\delta}$ ; 2)  $(\rho u \Delta h)_m$  and  $\bar{\delta}_T$ ; experiment: 3)  $(\rho u^2)_m$ ,  $\bar{\delta}$ ; 4)  $(\rho u \Delta h)_m$ ,  $\bar{\delta}_T$ .

Therefore, the radial dimensions of the jet increase with the superheating and differ appreciably from the radial dimensions for an isothermal jet ( $\theta_a = 1$ ) of incompressible fluid.

Figures 1 and 4 compare results for the transverse and axial parameters of jets of nitrogen, argon, and air with values from experiment [2] and values computed from measurements [8].

The calculations agree with experiment to within  $\sigma < 0.02$  for the axial parameters and within  $\sigma < 0.25$  for the effective thicknesses.

The coordinate for the initial section  $\bar{x}_0$  was chosen on the basis of experiment [2, 8].

One can estimate  $\bar{x}_0$  by means of a published relation [9] derived for slightly heated jets of variable composition:

$$\bar{x}_0 = 9/(\rho_m/\rho_a)^{0.5}. \quad (13)$$

Derivation of  $\bar{x}_0$  from (13) gives slightly exaggerated values because  $\bar{x}_0$  is affected by the turbulence, the uneven distribution of the gasdynamic parameters in the nozzle, and the high initial superheating. These factors reduce the length of the initial part to 3-4 times the radius of the nozzle [2].

Satisfactory agreement with experiment shows that the integral method widely applied to isothermal and slightly heated jets can also be applied to hot jets of variable composition provided that the self-modeling parameters are appropriately chosen, along with the equation of state for the gas mixture, the turbulent viscosity, etc.

#### LITERATURE CITED

1. A. S. Ginevskii, Theory of Turbulent Jets and Wakes [in Russian], Mashinostroenie, Moscow (1969).
2. I. A. Belov, I. P. Ginzburg, G. F. Gorshkov, and V. S. Terpigor'ev, in: Heat and Mass Transfer - V [in Russian], Vol. 1, Minsk (1976).
3. N. B. Vargaftik, Tables on the Thermophysical Properties of Liquids and Gases, Halsted Press (1975).
4. I. P. Ginzberg, Friction and Heat Transfer in the Motion of a Mixture of Gases [in Russian], Leningrad State Univ. (1975).
5. G. N. Abramovich, S. Yu. Krasheninnikov, A. N. Sekundov, and I. P. Smirnova, Turbulent Mixing of Gas Jets [in Russian], Nauka, Moscow (1974).

6. L. A. Vulis and V. P. Kashkarov, Theory of Jets of Viscous Fluids [in Russian], Nauka, Moscow (1974).
7. L. A. Vulis and L. P. Yarin, Fiz. Goreniya Vzryva, No. 2 (1974).
8. I. A. Bezmenov and V. S. Borisov, Izv. Akad. Nauk SSSR, Otd. Tekh. Nauk, Energ. Avtom., No. 4 (1961).
9. G. Kleinstein, Q. J. Appl. Math., 20, No. 1 (1962).

## PECULIARITIES OF THERMOPHYSICAL MEASUREMENTS OF THERMOELECTRIC MATERIALS

K. K. Semenyuk

UDC 536.2.083

This paper examines a method for direct measurement of the heat losses in determining the thermal conductivity of thermoelectric materials.

In [1] Harman proposed to determine the thermal conductivity of thermoelectric materials by measuring the temperature difference  $T_2 - T_1$  between the ends of a thermoelement, through which a current  $I$  was flowing, from the formula

$$\kappa = \frac{d}{s} \frac{eI(T_1 + T_2)}{2(T_2 - T_1)} (1 - \gamma). \quad (1)$$

In order to reduce the error  $\gamma$  due to thermal losses from the surface of the specimen, one uses quite long and fine thermocouples and current leads, and the measurements are conducted in vacuum on specimens of dimensions such that the condition  $\omega \ll 1$  holds [2, 3]. Below we examine the method of direct measurement of the correction term  $\gamma$  in Eq. (1). The method is based on the phenomenon that if the Peltier effect is used to create a heat flux through the thermoelement, the flux magnitude and direction can be controlled by varying the magnitude and direction of the electric current  $I$ .

We consider a thermoelement with current leads whose length satisfies the condition at infinity  $d_l \gg (r_{lx}l/\alpha_l)^{-1/2}$ . We assume also that the following conditions hold. 1) There is no temperature drop over the cross section of the thermoelement. This condition holds if  $(\alpha\delta/\kappa) \ll 1$ . 2) The thermoelectric parameters and the heat-transfer coefficient are independent of temperature. Then the heat-conduction equations for the thermoelement and the current leads in dimensionless form take the form

$$\frac{d^2\theta}{d\chi^2} - \omega^2(\theta - \theta_0) + v^2 = 0, \quad (2)$$

$$\frac{d^2\theta_{l1}}{d\chi^2} - \omega_{l1}^2(\theta_{l1} - \theta_0) + C_{l1}v^2 = 0, \quad (3)$$

$$\frac{d^2\theta_{l2}}{d\chi^2} - \omega_{l2}^2(\theta_{l2} - \theta_0) + C_{l2}v^2 = 0. \quad (4)$$

Here and below the subscripts 1 and 2 refer to the first (on the left in Fig. 1) and second faces, respectively, of the thermoelement. This means that the thermal conditions are different at the ends; and  $\theta_0$  is the dimensionless temperature of the surrounding medium.

We assume that for a single direction of current through the thermoelement the temperatures  $\theta_1' < \theta_2'$  are established at its ends. If the current direction is changed, then  $\theta_1'' > \theta_2''$ . Thus, Eqs. (2)-(4) can be solved by well-known methods with the following boundary conditions: for the first current direction

$$\theta(0) = \theta_{l1}(0) = \theta_1', \quad \theta(1) = \theta_{l2}(1) = \theta_2',$$

and for the second direction

$$\theta(0) = \theta_{l2}(0) = \theta_2', \quad \theta(1) = \theta_{l1}(1) = \theta_1'.$$

An additional condition for  $\theta_{l1}$  and  $\theta_{l2}$  is that the heat flux at infinity is zero.

---

Chernovitskii State University. Translated from Inzhenerno-Fizicheskii Zhurnal, Vol. 36, No. 5, pp. 891-895, May, 1979. Original article submitted February 13, 1978.